

# Neutrino nucleosynthesis in core-collapse Supernova explosions

A. Sieverding<sup>1,a</sup>, L. Huther<sup>1</sup>, G. Martínez-Pinedo<sup>1,2</sup>, K. Langanke<sup>2</sup>, and A. Heger<sup>3</sup>

<sup>1</sup>*Institut für Kernphysik (Theoriezentrum), Technische Universität Darmstadt, Schlossgartenstraße 2, 64289 Darmstadt, Germany*

<sup>2</sup>*Gesellschaft für Schwerionenforschung Darmstadt, Planckstr. 1, D-64259 Darmstadt, Germany*

<sup>3</sup>*Monash Centre for Astrophysics, School of Physics and Astronomy, Monash University, Victoria 3800, Australia*

**Abstract.** The neutrino-induced nucleosynthesis ( $\nu$  process) in supernova explosions of massive stars of solar metallicity with initial main sequence masses between 15 and 40  $M_{\odot}$  has been studied. A new extensive set of neutrino-nucleus cross-sections for all the nuclei included in the reaction network is used and the average neutrino energies are reduced to agree with modern supernova simulations. Despite these changes the  $\nu$  process is found to contribute still significantly to the production of the nuclei  ${}^7\text{Li}$ ,  ${}^{11}\text{B}$ ,  ${}^{19}\text{F}$ ,  ${}^{138}\text{La}$  and  ${}^{180}\text{Ta}$ , even though the total yields for those nuclei are reduced. Furthermore we study in detail contributions of the  $\nu$  process to the production of radioactive isotopes  ${}^{26}\text{Al}$ ,  ${}^{22}\text{Na}$  and confirm the production of  ${}^{92}\text{Nb}$  and  ${}^{98}\text{Tc}$ .

## 1 Introduction

Core-Collapse-Supernova explosions are among the most energetic events known to astronomers and mark the end of the live of massive stars. The conditions created by the passage of the supernova shockwave through the chemically enriched layers of massive stars allow for important nucleosynthesis processes to occur which are crucial for the enrichment of the interstellar medium and chemical evolution of the universe. A major part of the energy released by the core-collapse leaves the stellar core in the form of neutrinos of all flavors.

Those neutrinos can interact with the shock-heated material and affect the nucleosynthesis. In recent years multi-dimensional supernova simulations have given new insights concerning the neutrino radiation. Neutrinos with energies of the order of 10 MeV can lead to nuclear excitations beyond the particle separation threshold, affecting the chemical composition and density of free nucleons. Furthermore, electron neutrinos and electron antineutrinos can be captured by nuclei, leading to the inverse process of  $\beta$ -decay.

Following the approach of previous studies we choose a parametrized supernova model as described in reference [1] which allows a exploration of the parameter space of the neutrino properties and the explosion. The key ingredient of the explosive nucleosynthesis is the peak temperature of the shock heated material. This is estimated by an analytic expression that has been shown to agree quite well

<sup>a</sup>e-mail: [asiever@theorie.ikp.physik.tu-darmstadt.de](mailto:asiever@theorie.ikp.physik.tu-darmstadt.de)

**Table 1.** Production factors relative to solar abundances from reference [6], normalized to  $^{16}\text{O}$  production. Shown are the results obtained without neutrinos, with our choice of neutrino temperatures (“Low energies”:  $T_{\nu_e} = 2.8 \text{ MeV}$ ,  $T_{\bar{\nu}_e} = T_{\bar{\nu}_{\mu,\tau}} = T_{\nu_{\mu,\tau}} = 4.0 \text{ MeV}$ ), and with the choice of ref. [7] (“High energies”:  $T_{\nu_e} = T_{\bar{\nu}_e} = 4.0 \text{ MeV}$ ,  $T_{\nu_{\mu,\tau}} = T_{\bar{\nu}_{\mu,\tau}} = 6.0 \text{ MeV}$ ) for a  $25 M_{\odot}$  progenitor model.

Star	Nucleus	no $\nu$	Low energies	High energies
$15 M_{\odot}$	$^7\text{Li}$	0.001	0.28	2.54
	$^{11}\text{B}$	0.007	1.43	6.13
	$^{15}\text{N}$	0.67	0.68	0.79
	$^{19}\text{F}$	1.02	1.14	1.31
	$^{138}\text{La}$	0.07	0.67	1.18
	$^{180}\text{Ta}$	0.07	1.14	1.81
$25 M_{\odot}$	$^7\text{Li}$	0.0005	0.11	0.55
	$^{11}\text{B}$	0.003	0.80	2.61
	$^{15}\text{N}$	0.08	0.10	0.13
	$^{19}\text{F}$	0.06	0.24	0.43
	$^{138}\text{La}$	0.03	0.63	1.14
	$^{180}\text{Ta}$	0.14	1.80	2.81

with hydrodynamical simulations [2]. The decrease of temperature and density are modeled to be exponential on a density dependent timescale. Neutrinos are assumed to have Fermi-Dirac spectra with chemical potential  $\mu_{\nu} = 0$ , characterized by a neutrino temperature  $T_{\nu}$ , related to the average energy by  $\langle E_{\nu} \rangle \approx 3.14 T_{\nu}$ . Neutrino luminosities are modeled with an exponential decrease on the timescale of 3 s. A total energy of  $10^{53}$  erg is distributed equally among the 6 neutrino flavors, leading to number fluxes according to the average energy of the prescribed to the corresponding neutrino type.

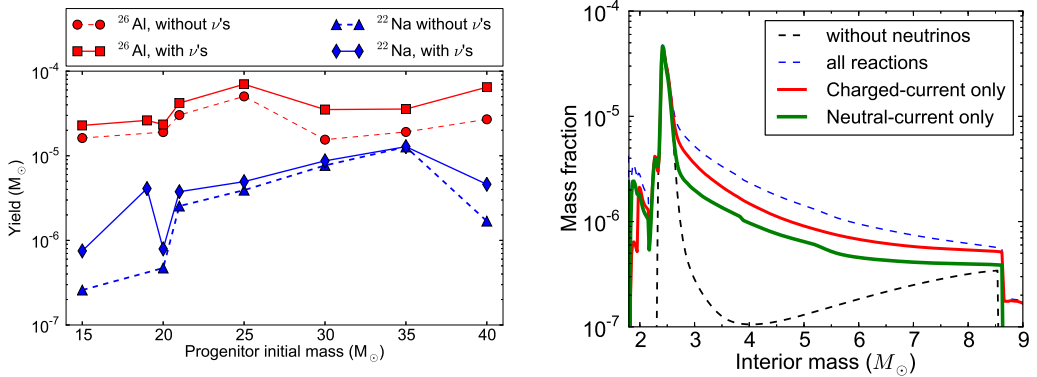
Our set of neutrino-nucleus cross-sections has been calculated for both, charged- and neutral-current reactions, based on Random Phase Approximation (RPA) [3]. Spallation products in the case of states above particle separation threshold are computed based on statistical models [4].

We use solar metallicity supernova progenitors calculated by A. Heger et al. [5], with main sequence masses ranging between 15 and  $40 M_{\odot}$ . The stellar models have been evolved up to core-collapse, providing the initial conditions and composition for the further evolution parametrized as stated above.

## 2 Canonical $\nu$ process nuclei

The  $\nu$  process is known to have significant effects on the production of  $^7\text{Li}$ ,  $^{11}\text{B}$ ,  $^{19}\text{F}$ ,  $^{138}\text{La}$  and  $^{180}\text{Ta}$  [1, 7]. Previous studies of neutrino nucleosynthesis have assumed average neutrino energies of  $\langle E_{\nu_e, \bar{\nu}_e} \rangle = 12.6 \text{ MeV}$ ,  $\langle E_{\nu_x} \rangle = 18.8 \text{ MeV}$ , where  $\nu_x$  corresponds to  $\nu_{\mu}$ ,  $\bar{\nu}_{\mu}$ ,  $\nu_{\tau}$  and  $\bar{\nu}_{\tau}$  [7]. Using instead significantly reduced values of  $\langle E_{\nu_e} \rangle = 8.8 \text{ MeV}$ ,  $\langle E_{\bar{\nu}_e, \nu_x} \rangle = 12.6 \text{ MeV}$  as suggested by detailed simulations e.g. in references [8, 9] we still see a significant increase in the production of  $^7\text{Li}$ ,  $^{11}\text{B}$ ,  $^{19}\text{F}$ ,  $^{138}\text{La}$  and  $^{180}\text{Ta}$  due to neutrino-induced reactions (see Table 1).

$^7\text{Li}$  is produced robustly in the lower He shell, where neutrino spallation of  $^4\text{He}$  leads to the presence of  $^3\text{He}$  and  $^3\text{H}$ , that can react with the very abundant  $\alpha$  particles to produce  $^7\text{Li}$ , mostly as  $^7\text{Be}$  which decays with a half-life of 53 days.  $^7\text{Li}$  cannot be produced up to the full solar abundance which confirms the role of cosmic-ray spallation for its production. Our studies have shown, that especially  $^{11}\text{B}$  is very sensitive to the included neutrino reactions as well as to the description of the thermodynamic



(a)  $^{26}\text{Al}$  yield for a set of progenitor stars. The largest enhancement can be found for the 30 and 35  $M_\odot$  progenitors. (b)  $^{26}\text{Al}$  Mass fraction for the 35  $M_\odot$  progenitor star for calculations including either only charged- or neutral current neutrino interactions.

**Figure 1.** The production of the radioactive isotopes  $^{26}\text{Al}$  and  $^{22}\text{Na}$  are increased by neutrino-induced reactions. We can disentangle neutral-current and charged-current contributions and see that in some cases charged-current reactions dominate.

conditions. The production of  $^{11}\text{B}$  has contributions from all the major shells. It can be produced via  $^{16}\text{O}(\nu, \nu' \alpha n/p)$  in the O/Ne layers. The neutral current spallation reactions  $^{12}\text{C}(\nu, \nu' n/p)$  as well as the charged current channel  $^{12}\text{C}(\nu_e, e^-)^{12}\text{N}(\gamma, p)$  contribute in the C/O shell of the star and in the He shell  $^7\text{Li}(\alpha, \gamma)$  is important.

Due to the large number of contributing neutrino channels the yield is very sensitive to the employed rates and because of charged particle reactions and photodissociation that are involved, the production is quite sensitive to temperature. Furthermore, there is a major contribution to the  $^{11}\text{B}$  yield below 1.6  $M_\odot$  of enclosed mass which is potentially accreted onto the PNS.

In table 1, it can be seen, that the the 15  $M_\odot$  progenitor model overproduces  $^{19}\text{F}$  even without neutrinos mainly via the reaction chain  $^{18}\text{O}(p, \alpha)^{15}\text{N}(\alpha, \gamma)^{19}\text{F}$  operating on  $^{18}\text{O}$  at the lower edge of the He shell. Due to the stellar structure this process does not work for the more massive progenitor models like the 25  $M_\odot$  model shown in Table 1. The production of  $^{19}\text{F}$  is very sensitive to the temperature that is reached in the region where  $^{18}\text{O}$  is present. For the more massive progenitor stars it is the neutrino-induced reaction  $^{20}\text{Ne}(\nu, \nu' p)^{19}\text{F}$ , as originally suggested by Woosley and Haxton [10], that leads to a significant increase of the production, even though the whole solar abundance cannot be produced. The tendency for less massive stars to produce  $^{19}\text{F}$  via nuclear reactions also appears for progenitor models from reference [11].

The Gamow-Teller parts of the reactions  $^{138}\text{Ba}(\nu_e, e^-)^{138}\text{La}$  and  $^{180}\text{Hf}(\nu_e, e^-)^{180}\text{Ta}$  are constrained by electron scattering data [12], and despite the low electron neutrino energies we see a significant production of these two odd-odd nuclei, which are most likely very important to explain their presence in the solar system. For  $^{180}\text{Ta}$  it is important to take into account, that only the meta stable excited state survives. In thermal equilibrium about 40% of the total yield of  $^{180}\text{Ta}$  could survive in this state [13].

A direct comparison between the present results and the results of reference [7] can be misleading, since differences appear due to the different treatment of hydrodynamic variables. Work to disentangle changes due to different neutrino interactions from changes due to the hydrodynamics is

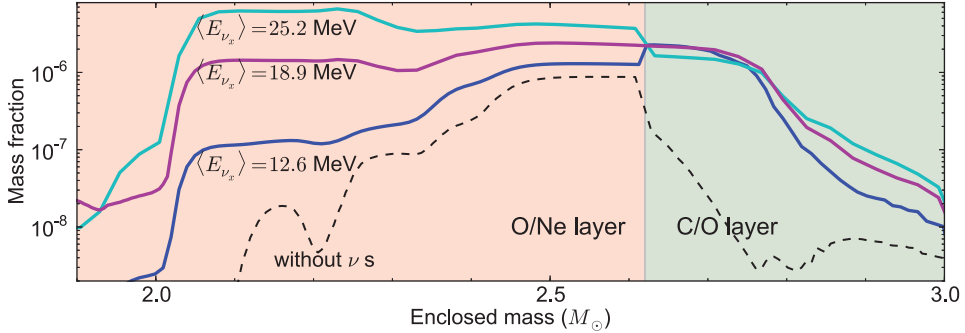


**Figure 2.**  $^{22}\text{Na}$  mass fraction for a  $15 M_{\odot}$  progenitor with different energies for  $\nu_{\mu}, \bar{\nu}_{\mu}, \nu_{\tau}, \bar{\nu}_{\mu}$ , abbreviated as  $\nu_x$ . The neutral-current contribution in the O/Ne shell is quite sensitive to the neutrino energy. Low energies give more importance to the charged-current contribution from the C/O shell.

in progress.

### 3 Impact on radioactive nuclei

Observations of  $\gamma$ -rays allow direct access to the production of  $^{26}\text{Al}$  in the galaxy. Supernova explosions are assumed to give a significant contribution to the overall abundance of  $^{26}\text{Al}$  [11]. Previous studies have already reported an enhancement of the production of  $^{26}\text{Al}$  by 30% to 50% [14] due to neutrinos. This effect is largely due to neutral-current spallation reactions that increase the abundance of free protons, enhancing capture reactions on  $^{25}\text{Mg}$  in the Oxygen-Neon shell. Figure 1(a) shows the yield of  $^{26}\text{Al}$  and  $^{22}\text{Na}$  for the set of progenitor stars we have used. The  $20 M_{\odot}$  progenitor sticks out, because it does not show the smallest change due to neutrinos. This is because this progenitor model suffers a convective merging of the O/Ne and C/O shells before the collapse. This episode mixes large amounts of  $^{22}\text{Ne}$  and  $^{26}\text{Mg}$  into the hotter regions below, where they act as neutron sources via (p,n) reactions. Hence, the  $20 M_{\odot}$  model is enriched in  $^{26}\text{Al}$  and  $^{22}\text{Na}$  already prior to the explosion, while the important seeds,  $^{26}\text{Mg}$  and  $^{22}\text{Ne}$  are destroyed.

We even find an increase in the production of  $^{26}\text{Al}$  of up to a factor of 2 for the  $30$  and  $35 M_{\odot}$  progenitor models. Especially in those cases the charged-current reaction  $^{26}\text{Mg}(\nu_e, e^-)^{26}\text{Al}$  is found to be the dominating channel for the increased production. The proton capture on  $^{25}\text{Mg}$  is quite sensitive to temperature and its peak that can be seen in Figure 1(b) is governed by the competition with a further proton capture. The charged current-channel however can operate with similar efficiency in the whole O/Ne and C/O shell, where  $^{26}\text{Mg}$  is present.

The uncertainties in the nuclear reaction rates that are involved in the production of  $^{26}\text{Al}$  give rise to a variation of a factor 3 in the  $^{26}\text{Al}$  production [15]. Since the neutrino interactions can induce changes of similar magnitude this emphasizes the need to constrain neutrino-nucleus cross-sections by experimental data.

The decay of  $^{22}\text{Na}$  is relevant for the description of supernova lightcurves [16]. In our calculations the production of  $^{22}\text{Na}$  is increased up to a factor of 3, mainly due to increased proton captures on  $^{22}\text{Ne}$  and  $^{22}\text{Ne}(\nu_e, e^-)^{22}\text{Na}$ . Figure 2 shows the distribution of the  $^{22}\text{Na}$

mass fraction for a  $15 M_{\odot}$  star. We can clearly distinguish the neutral-current and charged-current contributions. In The O/Ne shell, there is very little  $^{22}\text{Ne}$  present because it is destroyed in C-burning. Even though there is also  $^{21}\text{Ne}$  available for proton captures, but due to the lower temperature and the presence of  $^{22}\text{Ne}$ , the larger charged-current cross-section dominates.

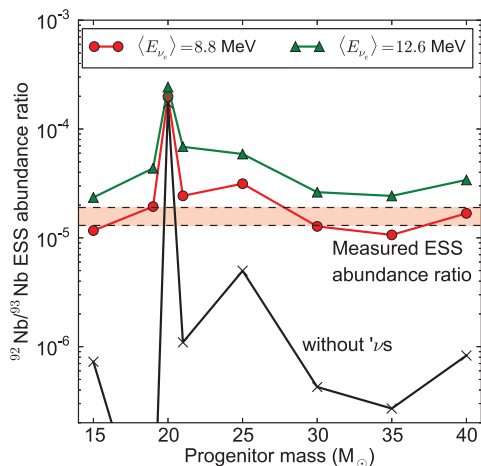


**Figure 3.**  $^{92}\text{Nb}/^{93}\text{Nb}$  abundance ratio in the early solar system estimated with a uniform production over 10 Gyr with the yields of the different progenitor models.

tope  $^{36}\text{Cl}$  which might be relevant to explain the existence of  $^{36}\text{Cl}$  in the early solar system, as inferred from meteoritic data. The characteristic  $\gamma$ -rays from the decay of  $^{44}\text{Ti}$  and  $^{60}\text{Fe}$  are also used as tracers for active nucleosynthesis sites [11, 19]. The effect of neutrino interactions on the yields of  $^{44}\text{Ti}$  and  $^{60}\text{Fe}$  have been found to be at most 2% in the case of  $^{44}\text{Ti}$  and even less for  $^{60}\text{Fe}$ .

$^{44}\text{Ti}$  is mostly produced in the deep interior close to the PNS where in an  $\alpha$ -rich freeze-out. At such high temperatures, charged particle reactions and photon-induced reaction dominate over any contribution from the  $\nu$  process.  $^{60}\text{Fe}$  is present in the C/O and O/Ne shells before the supernova shock arrives and it is hardly affected by the shock passage.  $^{60}\text{Fe}$  can be produced by a sequence of neutron captures starting  $^{58}\text{Fe}$ . However, the additional neutrons provided by neutrino-spallation cannot make a difference because they are preferentially captured by the more abundant nuclei.

## 4 Conclusions

We have studied the  $\nu$  process in core collapse supernovae for stars with initial masses between 15 and  $40 M_{\odot}$  with an extended set of neutrino-nucleus interaction cross-sections and reduced neutrino energies in agreement with modern supernova simulations. We find that the general features of the  $\nu$  process can still appear and we have identified key reactions and sensitivities for the production of radioactive isotopes.  $^{26}\text{Al}$  and  $^{22}\text{Na}$  are found to be affected by factors between 1.4 and 3. Due to the reduced neutrino energies we find a general increase in the relative importance of charged-current

In total we find also for  $^{22}\text{Na}$  an increase of the relative importance of charged-current channels.

We can also confirm significant contributions of the  $\nu$  process to the production of  $^{92}\text{Nb}$  and  $^{98}\text{Tc}$  due to electron neutrino absorption on the corresponding isobars, as also discussed in [17].

Indication for  $^{92}\text{Nb}$  has also been found in meteorites and the abundance ratio  $^{92}\text{Nb}/^{93}\text{Nb}$  in the early solar system has been estimated to be approximately  $10^{-5}$  [18]. We can estimate the early solar system abundance with a uniform production model  $^{92}\text{Nb}/^{93}\text{Nb} \approx P(^{92}\text{Nb})/P(^{93}\text{Nb}) \times 2\tau/10\text{Gyr}$  with the decay time  $\tau = 30\text{Myr}$  for  $^{92}\text{Nb}$  and the production yields  $P(^{92}\text{Nb})$  and  $P(^{93}\text{Nb})$  from our calculations. The results is shown if Figure 3 and we find a reasonably good agreement with the data that is difficult to achieve without taking into account neutrino interactions. Furthermore, we find a significant enhancement of the production of the short-lived radioisotope

reactions, in these cases especially electron neutrino capture on  $^{26}\text{Mg}$  and  $^{22}\text{Ne}$ .  $^{92}\text{Nb}$  is affected even more and the yields are compatible with measurement of meteoritic material. In order to make reliable comparisons between calculated supernova nucleosynthesis and observations, it is necessary to find more experimental constraints on the relevant cross sections.

## References

- [1] S.E. Woosley, D.H. Hartmann, R.D. Hoffman, W.C. Haxton, *ApJ***356**, 272 (1990)
- [2] S.E. Woosley, A. Heger, T.A. Weaver, *Reviews of Modern Physics* **74**, 1015 (2002)
- [3] E. Kolbe, K. Langanke, G. Martínez-Pinedo, P. Vogel, *Journal of Physics G Nuclear Physics* **29**, 2569 (2003)
- [4] L. Huther, Ph.D. thesis, TU Darmstadt, Darmstadt, Germany (2013)
- [5] T. Rauscher, A. Heger, R.D. Hoffman, S.E. Woosley, *ApJ***576**, 323 (2002)
- [6] K. Lodders, *ApJ***591**, 1220 (2003)
- [7] A. Heger, E. Kolbe, W.C. Haxton, K. Langanke, G. Martínez-Pinedo, S.E. Woosley, *Physics Letters B* **606**, 258 (2005)
- [8] T. Fischer, S.C. Whitehouse, A. Mezzacappa, F.K. Thielemann, M. Liebendörfer, *A&A***499**, 1 (2009)
- [9] L. Hüdepohl, B. Müller, H.T. Janka, A. Marek, G.G. Raffelt, *Physical Review Letters* **104**, 251101 (2010)
- [10] S.E. Woosley, W.C. Haxton, *Nature***334**, 45 (1988)
- [11] M. Limongi, A. Chieffi, *ApJ***647**, 483 (2006)
- [12] A. Byelikov, T. Adachi, H. Fujita, K. Fujita, Y. Fujita, K. Hatanaka, A. Heger, Y. Kalmykov, K. Kawase, K. Langanke et al., *Physical Review Letters* **98**, 082501 (2007)
- [13] D. Belic, C. Arlandini, J. Besserer, J. de Boer, J.J. Carroll, J. Enders, T. Hartmann, F. Käppeler, H. Kaiser, U. Kneissl et al., *Physical Review Letters* **83**, 5242 (1999)
- [14] F.X. Timmes, S.E. Woosley, D.H. Hartmann, R.D. Hoffman, T.A. Weaver, F. Matteucci, *ApJ***449**, 204 (1995)
- [15] C. Iliadis, A. Champagne, A. Chieffi, M. Limongi, *ApJS***193**, 16 (2011)
- [16] F.K. Thielemann, M.A. Hashimoto, K. Nomoto, *ApJ***349**, 222 (1990)
- [17] M.K. Cheoun, E. Ha, T. Hayakawa, S. Chiba, K. Nakamura, T. Kajino, G.J. Mathews, *Phys. Rev. C***85**, 065807 (2012)
- [18] M. Schönbachler, M. Rehkämper, A.N. Halliday, D.C. Lee, M. Bourot-Denise, B. Zanda, B. Hattendorf, D. Günther, *Science* **295**, 1705 (2002)
- [19] B.W. Grefenstette, F.A. Harrison, S.E. Boggs, S.P. Reynolds, C.L. Fryer, K.K. Madsen, D.R. Wik, A. Zoglauer, C.I. Ellinger, D.M. Alexander et al., *Nature***506**, 339 (2014)